TECHNICAL REPORT

NO. 8

HIGH RESOLUTION EMISSION VEGARD-KAPLAN BANDS OF NITROGEN

R. E. Miller

The Johns Hopkins University

Baltimore 18, Maryland

NASA RESEARCH GRANT
NsG 193-62

Prepared for

NATIONAL AERONAUTICS AND SPACE ADMINISTRATION

Washington, D. C.

1. Introduction

The Vegard-Kaplan band system of nitrogen is an electric dipole transition, occurring only by violating the approximate spin selection rule $\Delta S = 0$. This system is of importance since it fixes the absolute energy of the triplet states, i.e., the energy above the ground state of the molecule $X^1\Sigma (v = 0, J = 0)$. The upper level, $A\,^3\Sigma$, of these bands is also the lower level for the intense first positive system. Furthermore, these bands are observed in the spectrum of the night sky and of the aurora, and are now being sought in the spectrum of other planetary atmospheres.

These bands can be observed in the laboratory under rather special conditions of excitation and are the weakest of the known intercombination systems. Until now, no laboratory light source was known to emit these bands with sufficient intensity to be used with a high resolution spectrograph.

The $A^3\Sigma_u^+ - X^1\Sigma_g^+$ system of nitrogen was first observed by Vegard[1] and somewhat later by Kaplan.[2] Using an ordinary all-glass ozonizer at atmospheric pressure, Janin[3] was able to obtain a partial resolution of the rotational structure, and more recently Wilkinson[4] observed two bands in absorption.

None of the above investigations has completely resolved the rotational structure. The triplet splitting has not been resolved, and the absolute energy of the level is not accurately known.

2. Spectrograph

The instrument used was a 5-meter two-mirror vacuum Ebert type spectrograph, designed by Wm. G. Fastie, and constructed by the Jarrell Ash Company.[5] It employs a 5 x 10 inch Bausch and Lomb plane grating of 7500 grooves per inch and blazed at 5.9 μ in the first order. Thus, for example, the 2604 Å band was taken in the 23rd order, with a resolving power limited by the Doppler width of the lines, and a dispersion of about 1.5 cm^{-1} per mm. At these high orders the instrument has a relative aperture of about f/50.

In order to avoid overlapping orders, a small prism predisperser of suprasil quartz optics and 100 cm focal length was used.

The spectrograph was evacuated to about 5×10^{-5} mm Hg for all exposures.

3. Wavelength Standards

The wavelength reference source used for all exposures was the iron hollow cathode discharge tube.[6] The wavelengths used were mainly from measurements on this source performed in this laboratory.[7] Tests on the use of overlapping orders with this grating have shown no coincidence errors. The standard lines are generally known to better than 0.005 cm^{-1}, and the accuracy for sharp nitrogen lines of medium density is also of this order, as seen from the agreement of the combination relations.

The plate measurements were reduced with the aid of a computer program which consisted of a least squares fit to the grating equation appropriate for this spectrograph.

4. Light Source

There are several problems that must be overcome in order to obtain a source that will emit the Vegard-Kaplan bands with sufficient intensity.

a. Nitrogen of very high purity must be obtained. The chief troublesome impurity is oxygen, and the reason for this is two-fold. First, the oxygen combines with the nitrogen to form nitric oxide, which seems to be quite effective in quenching the V-K bands.[8] Second, the nitric oxide bands lie very close to the V-K bands, so that even when the V-K band heads are easily distinguishable, the overlapping of the two makes a fine structure analysis very difficult, if not impossible. Janin[3] has also found that mercury vapor is very effective in quenching these bands.

b. The nitrogen must be kept pure during the discharge, since the energetic electrons or ions that are present tend to knock

oxygen and other atoms out of the glass walls. Also, the outgassing of the electrodes can be a serious source of contamination.

c. The optimum source conditions must be found that will favor the weak V-K emission while disfavoring the stronger L-B-H and Second Positive systems, since these can also cause overlapping.

The gas used for these exposures was obtained from the Matheson Company in one-liter glass flasks (reagent grade, less than 4 ppm 0_2). Without further purification, however, the NO bands were found to be very strong. The final method used for purifying the gas made use of a 64% zirconium - 36% titanium alloy as a getter.

The purifying system and discharge tube was combined into an all-glass and quartz ultra-high vacuum system. The getter was outgassed by baking it at 1100°C for about twenty-four hours, and then the entire system was baked at 425°C for another twenty-four hours. This baking process was then repeated once or twice. The final vacuum usually attained was a few times 10^{-8} mm of mercury, which is the limit that the VG-IA ionization gauge can read, due to the photoelectron current. The nitrogen gas was then introduced into the getter tube, which was now heated to about 800° C. After several hours the gas was permitted to flow into the discharge tube. The exact time that the nitrogen is in contact with the getter seems to be of little importance.

The final discharge tube was a quartz tube 32 mm in diameter and 65 cm in length. A quartz window was fused to one end, and an electrode of vacuum processed aluminum was placed about 5 cm from each end. The electrodes were in the form of hollow cylinders and their axes coincided with the axis of the quartz tube. Thus, the discharge was viewed through the front electrode. In this design there are no bends or constrictions, and the discharge is therefore kept from the walls of the tube as much as possible. The electrodes were thoroughly outgassed before baking. With this tube we have found that there was no increase in the concentration of NO, even after many weeks of continuous running.

Of the several different methods of excitation that were tried, the best seems to be a 60 cycle, high voltage discharge. The most intense V-K bands appeared at a pressure of approximately 3 mm of Hg and a

current of 5 milliamperes. Under these conditions, the discharge appeared blue in color and remained in the tube for a short time after the power had been turned off. In the literature, this blue afterglow is referred to as the NO afterglow; this seems to be incorrect, at least in this case, since the NO bands were practically nonexistent on the photographic plates even after the longest exposures.

It was also found that the addition of a small amount of xenon or helium increased some of the V-K bands slightly. For instance, xenon increased the intensity of the 3198 band, whereas helium favored the 2760 band. These rare gases can be easily purified by using uranium hydride as a getter.

With this light source, good exposures could be obtained in about 20 minutes with a 1-meter Eagle spectrograph which was used for survey work, and from 10 to 35 hours with the 5-meter spectrograph and prism predisperser. Kodak Tri-X film was used in the 1-meter Eagle and 103a-0 spectroscopic plates in the 5-meter instrument.

5. Analysis

5.1 Rotational Structure. The V-K system is a $^3\Sigma_u^+ - {}^1\Sigma_g^+$ transition, and thus each band consists of four branches. There is an R_2 branch ($\Delta J = +1$, $\Delta K = +1$), a P_2 branch ($\Delta J = -1$, $\Delta K = -1$), an R_3 branch ($\Delta J = 0$, $\Delta K = +1$), and a P_1 branch ($\Delta J = 0$, $\Delta K = -1$). The first two will hereafter be abbreviated to R and P, respectively. A schematic diagram of the rotational structure is given in Figure 1. As indicated in the figure, the three components of the $^3\Sigma_u^+$ state are designated by F_1, F_2, and F_3.

Table I gives both vacuum wavelengths and wavenumbers of the lines, with their classification, for the 0-4, 0-5, and 0-6 bands.

5.2 Molecular Constants. According to the theory developed by Kramers[9] and Schlapp,[10] the F_2 component is given by the equation for the ordinary nonrigid rotator, whereas the F_1 and F_3 components are given by more complicated equations containing additional terms. Thus, the rotational constants can be determined by an analysis of

the P and R branches only. The P_1 and R_3 branches have to be taken into account only for a discussion of the triplet splitting.

The combination differences

$$\Delta_2 F_0'(K) = R(K-1) - P(K+1)$$
$$= (4B_0' - 6D_0')(K + \tfrac{1}{2}) - 8D_0'(K + \tfrac{1}{2})^3$$

were obtained for the 0-4, 0-5, and 0-6 bands. From their mean values and the $\Delta_2 F_0'(K)/(K+\frac{1}{2})$ against $(K+\frac{1}{2})^2$ plot, the rotational constants

$$B_0' = 1.4459 \pm 0.0002 \text{ cm}^{-1}$$
$$D_0' = (6.15 \pm 0.2) \times 10^{-6} \text{ cm}^{-1}$$

were obtained. This value of B_0' agrees very well with the value 1.4457 obtained by Dieke and Heath,[11] but the value D_0' differs slightly from the value 5.83×10^{-6} obtained by Carroll.[12] Both of the previous values were obtained from analyses of the first positive system.

When there is one state, as in the present case ($v' = 0$), for which the combination differences are known with particular accuracy, greater accuracy for the other rotational constants can be obtained by using the following method rather than again using combination differences.

The differences between the rotational constants of the upper and lower states, that is, $(B' - B'')$ and $(D' - D'')$, can be determined by making use of the equation

$$\tfrac{1}{2}[P(K) + R(K)] = (\nu_0 + B' - 2D') + (B' - B'' - 6D')K(K+1) - (D' - D'')K^2(K+1)^2$$

By using the observed values of $[P(K)+R(K)]$ and the calculated values of $(\nu_0 + B' - 2D')$, the quantities

$$\frac{\tfrac{1}{2}[P(K) + R(K)] - (\nu_0 + B' - 2D')}{K(K+1)}$$

are calculated and plotted against $K(K+1)$. A straight line is obtained,

four branches for each band.

An inaccuracy in the intensities is caused by the narrowness of the blaze of the grating at high orders. For example, the width of the blaze at $\frac{1}{4}$ the intensity of the maximum is only about 130 A in the 23rd order. Thus, there can be a considerable intensity variation from one end to the other of a 25 A band, if the exposure was taken on a rapidly changing part of the blaze curve. However, this has little effect on the relative intensities of closely spaced lines such as those due to the triplet splitting.

It is interesting to note that the intensity of the R_3 branch is only slightly less and the P_1 branch slightly more than the R and P branches, respectively. This disproves Janin's[3] conclusion that the reason the triplet splitting was not resolved on his plates was that the P_1 and R_3 branches were probably much weaker than the P and R branches.

The distribution of the molecules over the different rotational levels in the $A\,^3\Sigma_u^+$ state will correspond to thermal equilibrium at a certain effective temperature, due to the numerous collisions that the molecules undergo before radiating. Therefore, we can make use of the Boltzman factor $e^{-E/kT}$ and obtain the following relation for the intensity distribution in the rotational structure as a function of temperature;

$$\ln \frac{I_{em}}{K' + K'' + 1} = A - \frac{B_{v'}\, K'(K'+1)h\nu}{kT}$$

By plotting $\ln (I/K'+K''+1)$ versus $K'(K'+1)$ for the 0-6 band and using the value of B_0' obtained above, we find the effective temperature of the source to be 335°K.

Exposures were also taken with the light source at a temperature of 77°K, but no enhancement of the Vegard-Kaplan system was observed.

The rotational temperature of 335°K corresponds to that found in auroras at a height of 125 km, which is the approximate height of greatest aurora frequency.[15] This laboratory has previously measured the V-K emissions in an aurora at this height using a rocket spectrophotometer.[16-17]

5.5 Triplet Splitting of the $A\,^3\Sigma$ State. Several different interactions must be taken into account for an analysis of the triplet splitting. The magnetic moment which is produced by the molecular rotation causes a slight magnetic coupling between $\vec{S}$ and $\vec{K}$. This coupling produces a slight splitting of the levels with different J and equal K, and increases with increasing K. The spin-spin interaction of the uncompensated electrons causes an additional splitting and was shown by Kramers[9] to be equivalent to an interaction between $\vec{S}$ and the figure axis. A further cause of the fine structure has been given by Hebb.[18] This is the magnetic moment which arises from the orbital angular momentum and which in a Σ state precesses at right angles about the internuclear axis. Thus, this magnetic moment also interacts with the total spin $\vec{S}$.

Taking the above interactions into account, the splitting for a $^3\Sigma$ state is given by

$$F_1(K')-F_2(K') = (2K'+3)B_\nu - \lambda - [(2K'+3)^2 B_\nu^2 + \lambda^2 - 2\lambda B_\nu]^{1/2} + \gamma(K'+1)$$
$$F_3(K')-F_2(K') = -(2K'-1)B_\nu - \lambda - [(2K'-1)^2 B_\nu^2 + \lambda^2 - 2\lambda B_\nu]^{1/2} - \gamma K'$$

The constant γ is a measure of the interaction between the spin $\vec{S}$ and the rotational magnetic moment, and the constant λ is a measure of the other two interactions mentioned above.

The observed values of $F_1(K')-F_2(K')$ and $F_3(K')-F_2(K')$ are given in Table V along with the computed values obtained by using the above equations and setting $\lambda = -1.33$ and $\gamma = -0.003$.

The variation of the triplet splitting with quantum number K' is shown in Fig. 2, which also shows the very good agreement that exists between theory and experimental results.

The presence of the constant λ is an indication that the $A\,^3\Sigma_u^+$ state does not belong completely to Hund's case b, and the smallness of the constant γ indicates that there is only a very weak coupling between the spin $\vec{S}$ and the magnetic moment, due to molecular rotation.

5.6 Absolute Energy. The absolute energy of the triplet levels in nitrogen can now be obtained by adding to the values of the band origins, obtained above, the corresponding energy of the v = 4, 5, and 6 vibrational levels of the $X'\,\Sigma$ ground state. These can be obtained from the

more intense Lyman-Birge-Hopfield system. At present, however, the accuracy of the latter are about a hundred times less than the V-K band origins. In order to correct this situation, a high resolution analysis of the L-B-H system has been undertaken.

Acknowledgements

The author is grateful to Professor G. H. Dieke for his advice and assistance in this work and for his careful reading of the manuscript; to Dr. H. M. Crosswhite for his help with the computer program and wavelength standards; and to Mr. F. Maiolatesi for assistance with the glasswork.

Table I

Bands of the Vegard-Kaplan System

(0-4) Band			
λ(Å)	I	$\nu(cm^{-1})$	Classification
2462.1565	3.5	40 614.801	R_3 2
2.1918	1.7	614.220	R_3 1
2.2176	2.5	613.792	R_3 4
2.2591	6.8	613.105	R 3
2.3134	7.1	612.212	R 4
2.3337	2.5	611.878	R_3 5
2.4252	2.9	610.369	R 5
2.4371	2.1	610.175	R 0
2.5033	4.2	609.080	R_3 6
2.5944	7.1	607.579	R 6
2.7312	2.1	605.324	R_3 7
2.8217	2.9	603.835	R 7
3.0168	6.2	600.613	R_3 8
3.0812	3.9	599.556	P_1 2
3.1069	5.0	599.130	R 8
3.1355	1.7	598.658	P 2
3.4224	2.1	593.931	P_1 3
3.4493	2.9	593.486	R 9
3.5100	2.9	592.487	P 3
3.7628	4.5	588.322	R_3 10
3.8244	1.1	587.310	P_1 4
3.8497	5.9	586.887	R 10
3.8907	2.9	586.215	P 4
4.2205	1.7	580.785	R_3 11
4.2865	2.9	579.697	P_1 5
4.3088	4.8	579.332	R 11
4.3548	1.7	578.575	P 5
4.7358	3.9	572.294	R_3 12
4.8051	9.1	571.157	P_1 6
4.8230	5.4	570.861	R 12
4.8758	4.5	569.996	P 6
5.3117	1.7	562.818	R_3 13
5.3833	3.9	561.639	P_1 7
5.3988	3.5	561.392	R 13
5.4548	2.5	560.466	R 7
5.9426	2.9	552.440	R_3 14
6.0190	10.0	551.184	P_1 8
6.0909	5.6	550.007	P 8
6.6335	1.7	541.086	R_3 15
6.7136	4.5	539.766	P_1 9

Table I, continued

(0-4) Band			
λ(Å)	I	$\nu(cm^{-1})$	Classification
2466.7856	2.5	40 538.580	P 8
7.3808	2.5	528.806	R_3 16
7.4656	12.9	527.411	P_1 10
7.5390	7.1	526.208	P 10
8.1847	2.1	515.605	R_3 17
8.2601	1.1	514.367	R 17
8.2755	4.5	514.117	P_1 11
8.3488	2.1	512.913	P 11
9.0573	2.1	501.287	R_3 18
9.1432	10.0	499.878	P_1 12
9.2180	4.5	498.649	P 12
9.9807	2.1	486.147	R_3 19
2470.0699	2.9	484.683	P_1 13
0.1454	2.1	483.440	P 13
1.0575	5.6	468.507	P_1 14
1.1318	3.5	467.289	P 14
2.1010	2.1	451.422	P_1 15
2.1765	1.7	450.187	P 15
2.2793	2.1	432.151	P 16
4.4406	1.0	413.173	P 17
5.5872	2.0	394.456	P_1 18
5.6615	1.0	393.244	P 19
(0-5 Band)			
2604.1778	5.5	38 399.834	R_3 2
4.2311	6.8	399.047	R_3 4
4.2868	4.9	398.228	R 3
4.2951	10.0	398.105	R 2
4.3227	1.3	397.699	R_3 0
4.3368	12.0	397.490	R 4
4.3467	7.6	397.346	R_3 5
4.3671	4.0	397.045	R 1
4.4504	6.2	395.818	R 5
4.5021	4.9	395.053	R 0
4.5243	7.9	394.726	R_3 6
4.6260	12.3	393.229	R 6
4.7629	4.6	391.209	R_3 7
4.8635	6.0	389.727	R 7
5.0636	9.3	386.778	R_3 8

Table I, continued

(0-5 Band)				
λ(Å)	I	ν(cm^{-1})	Classification	
2605.1634	12.6	38 385.308	R	8
5.2124	8.5	384.585	P_1	2
5.2772	2.0	383.632	P	2
5.4263	4.6	381.432	R_3	9
5.5249	5.8	379.980	R	9
5.5878	4.9	379.055	P_1	3
5.6573	2.5	378.030	P	3
5.8506	8.1	375.183	R_3	10
5.9490	11.0	373.735	R	10
6.0277	11.0	372.576	P_1	4
6.1029	6.2	371.469	P	4
6.3289	4.3	368.143	R_3	11
6.4356	4.6	366.572	R	11
6.5321	5.4	365.151	P_1	5
6.6094	3.6	364.015	P	5
6.8861	7.6	359.942	R_3	12
6.9838	9.6	358.502	R	12
7.0985	12.9	356.816	P_1	6
7.1779	8.5	355.648	P	6
7.4964	2.9	350.963	R_3	13
7.5946	4.3	349.518	R	13
7.7284	6.2	347.550	P_1	7
7.8085	4.6	346.373	P	7
8.1705	5.1	341.051	R_3	14
8.2687	6.8	339.607	R	14
8.4206	12.9	337.373	P_1	8
8.5018	9.8	336.181	P	8
8.9066	2.9	330.234	R_3	15
9.0046	3.6	328.794	R	15
9.1757	6.2	326.281	P_1	9
9.2574	5.1	325.081	P	9
9.7058	4.3	318.496	R_3	16
9.8037	4.9	317.056	R	16
9.9933	14.1	314.274	P_1	10
2610.0758	9.6	313.062	P	10
0.5561	1.3	306.014	R_3	17
0.6924	2.0	304.014	R	17
0.8736	5.1	301.355	P_1	11
0.9562	4.9	300.143	P	11
11.4922	2.9	292.284	R_3	18

Table I, continued

(0-5 Band)			
λ(Å)	I	ν(cm^{-1})	Classification
2611.5904	3.3	38 290.844	R 18
1.8167	10.2	287.524	P_1 12
1.8998	8.5	286.306	P 12
2.4786.	2.0	277.825	R_3 19
2.5634	2.0	276.583	R 19
2.8226	4.6	272.784	P_1 13
3.8918	7.8	257.130	P_1 14
3.9756	6.2	255.903	P 14
5.0242	2.5	240.563	P_1 15
5.1086	2.5	239.330	P 15
6.2202	4.9	223.080	P_1 16
6.3040	4.0	221.856	P 16
7.4795	2.0	204.693	P_1 17
7.5481	2.0	203.692	P 17
8.8024	2.0	185.393	P_1 18
8.8865	2.0	184.166	P 18
20.2701	1.6	164.005	P 19
(0-6 Band)			
2761.3667	3.0	36 213.951	R_3 3
1.3772	3.3	213.813	R_3 2
1.4175	7.8	213.284	R_3 4
1.4522	1.2	212.829	R_3 1
1.4893	5.4	212.343	R 3
1.5080	12.9	212.098	R 2
1.5353	17.8	211.740	R 4
1.5950	2.6	210.956	R 1
1.6502	7.1	210.233	R 5
1.7173	10.0	209.353	R_3 6
1.7484	6.3	208.945	R 0
1.8314	14.8	207.858	R 6
1.9669	5.1	206.080	R_3 7
2.0801	6.9	204.597	R 7
2.2361	0.7	202.552	P 1
2.2832	11.5	201.935	R_3 8
2.3954	15.9	200.463	R 8
2.5393	8.7	198.579	P_1 2
2.6088	2.3	197.669	P 2
2.6672	5.8	196.905	R_3 9
2.7782	6.9	195.449	R 9

Table I, continued

(0-6 Band)			
λ(Å)	I	$\nu(cm^{-1})$	Classification
2762.9538	5.8	36 193.149	P_1 3
3.0342	2.3	192.097	P 3
3.1170	11.0	191.010	R_3 10
3.2280	15.1	189.556	R 10
3.4379	13.5	186.810	P_1 4
3.5218	6.9	185.708	P 4
3.6348	5.1	184.230	R_3 11
3.7450	6.9	182.788	R 11
3.9908	6.9	179.569	P_1 5
4.0780	4.8	178.428	P 5
4.2196	10.0	176.577	R_3 12
4.3294	12.6	175.140	R 12
4.6119	16.6	171.442	P_1 6
4.7015	11.0	170.270	P 6
4.8718	3.9	168.042	R_3 13
4.9814	6.0	166.607	R 13
5.3011	9.1	162.425	P_1 7
5.3919	6.9	161.240	P 7
5.5910	8.1	158.637	R_3 14
5.7008	10.0	157.201	R 14
6.0584	19.5	152.526	P_1 8
6.1497	14.1	151.332	P 8
6.3697	4.2	148.459	R_3 15
6.4882	4.8	146.910	R 15
6.8828	10.0	141.754	P_1 9
6.9742	8.5	140.561	P 9
7.2330	6.6	137.180	R_3 16
7.3426	8.1	135.749	R 16
7.7756	20.0	130.094	P_1 10
7.8685	16.6	128.884	P 10
8.1558	3.5	125.135	R_3 17
8.2656	4.5	123.701	R 17
8.7360	10.0	117.561	P_1 11
8.8291	8.1	116.347	P 11
9.1475	4.2	112.197	R_3 18
9.2575	4.8	110.762	R 18
9.7641	19.5	104.157	P_1 12
9.8576	15.9	102.938	P 12
2770.3181	2.6	096.936	R 19
0.8608	8.3	089.866	P_1 13
0.9548	7.1	088.643	P 13

Table I, continued

(0-6 Band)			
λ(Å)	I	$\nu(cm^{-1})$	Classification
2771.3350	3.0	36 083.691	R_3 20
1.4457	3.9	082.250	R 20
2.0254	16.6	074.705	P_1 14
2.1197	13.8	073.479	P 14
2.6665	2.6	066.363	R 21
3.2583	8.3	058.668	P_1 15
3.3526	6.3	057.441	P 15
3.9053	3.3	050.256	R 22
4.5597	13.8	041.754	P_1 16
4.6540	10.2	040.529	P 16
6.0250	4.6	022.729	P 17
7.3695	8.3	005.291	P_1 18
7.4631	8.1	004.077	P 18
8.8784	3.9	35 985.751	P_1 19
8.9719	3.9	984.530	P 19
2780.4561	6.3	965.322	P_1 20
0.5500	5.8	964.106	P 20
3.8203	4.5	921.859	P_1 22
3.9152	3.5	920.634	P 22

Table II

Rotational Constants of the $X\ ^1\Sigma$ State

v	B"	D"
4	$1.9199 \pm 0.0003\ cm^{-1}$	$6.1 \pm 1.0 \times 10^{-6}\ cm^{-1}$
	(1.919 ± 0.001)	(5.5×10^{-6})
5	1.9024 ± 0.0002	$6.26 \pm 0.1 \times 10^{-6}$
	(1.9007 ± 0.0015)	(5.5×10^{-6})
6	1.8847 ± 0.0002	$6.2 \pm 0.3 \times 10^{-6}$
	(1.882 ± 0.0002)	(5×10^{-6})

The values in parentheses are those obtained from an analysis of the L-B-H system by Wilkinson and Houk[13] and Wilkinson.[14]

Table III

Band Origins for Three V-K Bands

Band	ν_0	
0 - 4	40 607.246	0.003 cm^{-1}
0 - 5	38 392.167	0.003
0 - 6	36 206.048	0.002

Table IV

ΔG Values Obtained from the Band Origins in Table III

v	ΔG	ΔG[13]
4	2 215.082 cm^{-1}	
5	2 186.119	2 187.7 cm^{-1}

Value in Column 3 is from Wilkinson and Houk.[13]

Table V

Triplet Splitting of the $A\,^3\Sigma$ State

K'	$F_1(K') - F_2(K')$		$F_3(K') - F_2(K')$	
	Observed Mean	Computed	Observed Mean	Computed
1	0.93 cm^{-1}	0.946 cm^{-1}	2.65 cm^{-1}	2.663 cm^{-1}
2	1.04	1.047	1.87	1.941
3	1.105	1.106	1.73	1.717
4	1.139	1.140	1.61	1.616
5	1.170	1.163	1.551	1.557
6	1.181	1.181	1.53	1.523
7	1.193	1.191	1.496	1.500
8	1.197	1.205	1.483	1.482
9	1.211	1.207	1.471	1.472
10	1.213	1.213	1.454	1.458
11	1.219	1.216	1.451	1.456
12	1.224	1.219	1.442	1.450
13	1.227	1.223	1.439	1.447
14	1.228	1.224	1.44	1.445
15	1.225	1.225	1.44	1.439
16		1.226	1.44	1.440
17	1.22	1.226	1.44	1.440

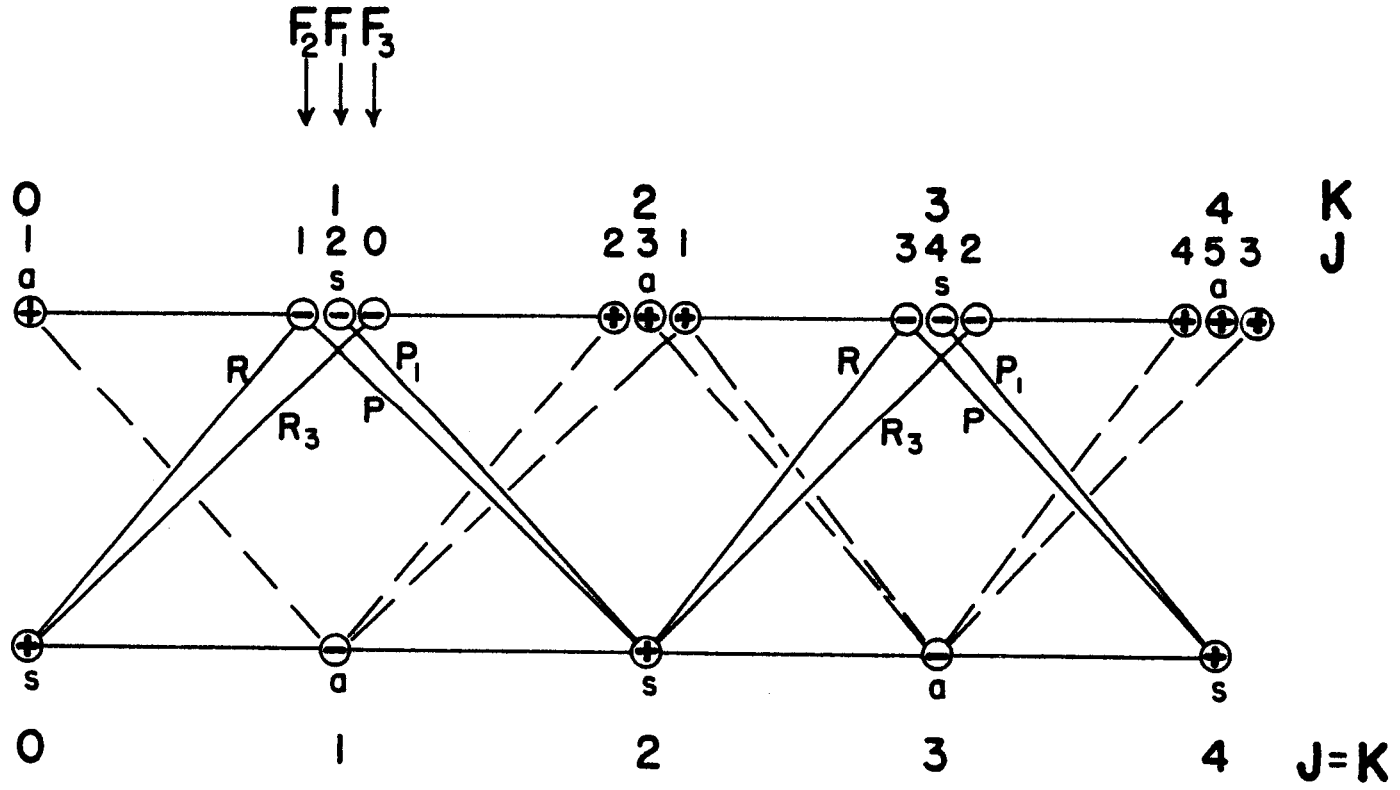

Figure 1. Schematic diagram of the rotational structure of the Vegard-Kaplan bands. The transition from antisymmetric rotational levels are weaker and are indicated by the broken lines.

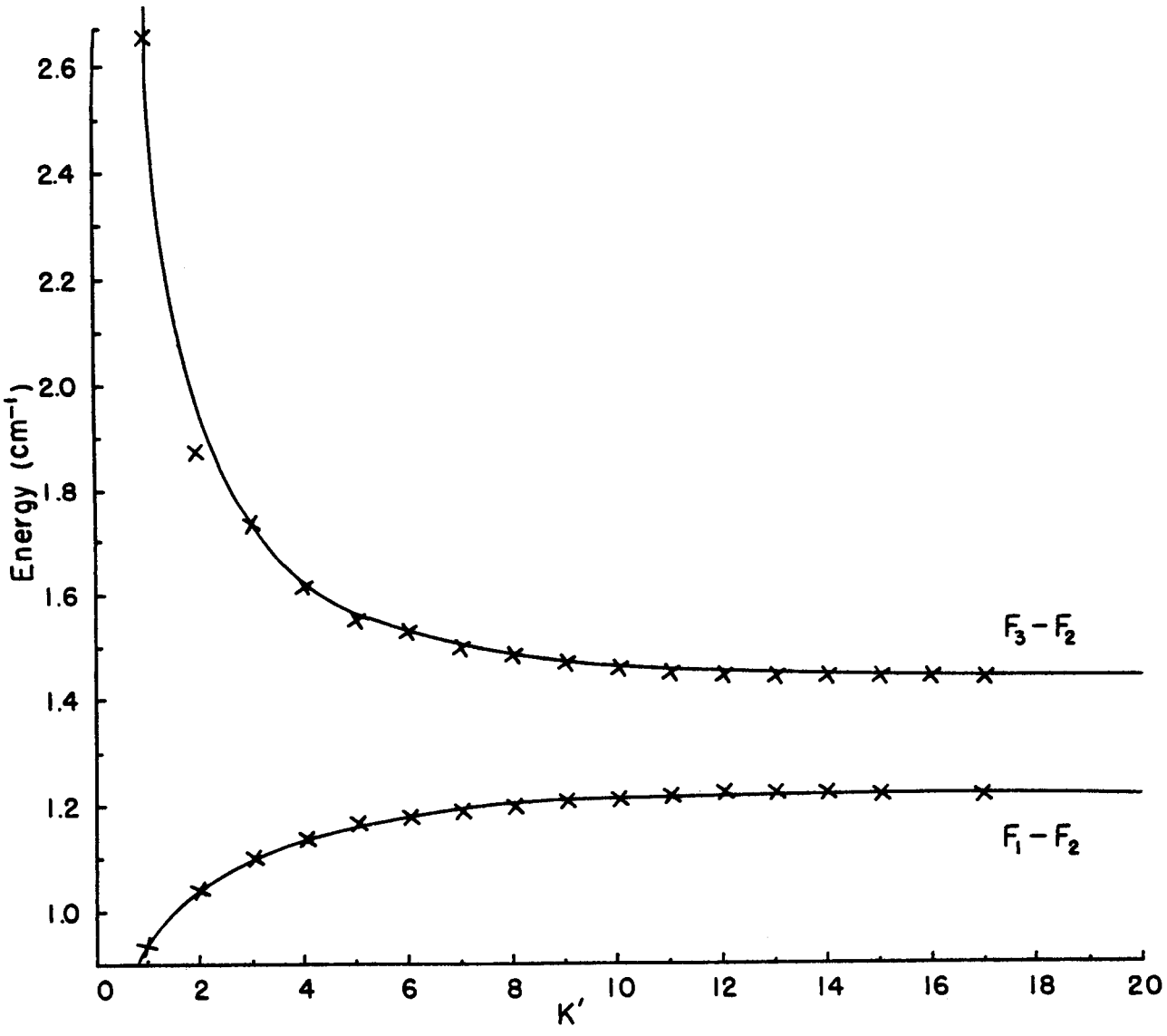

Figure 2. Splitting of the A $^3\Sigma$ state. The crosses are the experimentally observed points and the solid curves give the computed values.

References

1. L. Vegard, Z. Physik 75, 30 (1932)
2. J. Kaplan, Phys. Rev. 44, 947 (1933)
3. J. Janin, Ann. de Phys. (12) 1, 538 (1946)
4. P. G. Wilkinson, J. Chem. Phys. 30, 773 (1959)
5. G. H. Dieke and D. F. Heath, Proc. of the ICO Conf., Tokyo-Kyoto, Sept. 1964
6. H. M. Crosswhite, G. H. Dieke and C. S. Legagneur, J. Opt. Soc. Am. 45, 270 (1955)
7. Am. Inst. of Physics Handbook, 2nd ed., McGraw-Hill, 7-92
8. E. C. Zipf, Jr., J. Chem. Phys. 38, 2034 (1963)
9. H. A. Kramers, Zeits. f. Physik 53, 422 (1929)
10. R. Schlapp, Phys. Rev. 39, 806 (1932)
11. G. H. Dieke and D. F. Heath, Johns Hopkins Spectroscopic Report No. 17, Baltimore, Maryland, 1959
12. P. K. Carroll, Proc. Roy. Irish Acad. 54A, 369 (1952)
13. P. G. Wilkinson and N. B. Houk, J. Chem. Phys. 24, 528 (1956)
14. P. G. Wilkinson, Astrophys. J., 126, 1 (1957)
15. J. H. Brandy, Can. J. Phys. 42, 1793 (1964)
16. W. G. Fastie, H. M. Crosswhite and T. P. Markham, Ann. Geophys. 17, 109 (1961)
17. H. M. Crosswhite, E. C. Zipf, Jr., and W. G. Fastie, J. Opt. Soc. Amer. 52, 643 (1962)
18. M. H. Hebb, Phys. Rev. 49, 610 (1936)